

## OPERATING LIMITS OF AL-ALLOYED HIGH-LOW JUNCTIONS FOR BSF SOLAR CELLS

J. DEL ALAMO, J. EGUREN and A. LUQUE

Instituto de Energia Solar (E.T.S.I.T.), Universidad Politécnic de Madrid, Spain

(Received 15 May 1980; in revised form 10 September 1980)

**Abstract**—Experimental estimations of the effective surface recombination velocity of the high-low junction ( $S_{\text{eff}}$ ) and of the base diffusion length are carried out for Al-alloyed  $n^+pp^+$  bifacial cells and the results are presented in form of histograms. These results agree with calculated values of  $S_{\text{eff}}$  when the characteristics of the recrystallized Si layer and heavy doping effects are taken into account. It is concluded that thick Al layers and high alloying temperatures (over 800°C) are necessary to obtain low values of  $S_{\text{eff}}$ . This conclusion agrees with experimental results of other authors. Recommendations to avoid diffusion length degradation are given and the operating limits of the Al alloying technology are discussed.

### NOTATION

$A$	total area of the cell
$D$	diffusion coefficient of minority carriers
$E$	Si weight percentage of the Al-Si eutectic alloy
$F$	Si weight percentage of the liquid phase
$g$	generation rate of minority carriers
$g_b$	generation rate under back illumination
$g_f$	generation rate under front illumination
$I_o$	dark saturation current
$I_{scb}$	short-circuit current under back illumination
$I_{scf}$	short-circuit current under front illumination
$k$	Boltzmann constant
$L$	minority carrier diffusion length
$p_{Al}$	weight of deposited Al
$p_{Si}$	weight of recrystallized Si
$q$	electron charge
$n'$	excess electron concentration
$n_i$	intrinsic carrier concentration
$N_A$	acceptor concentration
$N_{ph}$	number of impinging photons per $\text{cm}^2$ and sec
$S_b$	back surface recombination velocity
$S_{\text{eff}}$	effective surface recombination velocity of the high-low junction
$T$	absolute temperature (°K)
$T_a$	annealing temperature (°C)
$V$	applied voltage
$V_{ocb}$	open-circuit voltage under back illumination
$V_{ocf}$	open-circuit voltage under front illumination
$W$	base thickness
$W_{n^+}$	$n^+$ -region thickness
$W_{p^+}$	$p^+$ -region thickness
$x$	coordinate
$\alpha$	absorption coefficient
$\rho_{Si}$	density of Si

### 1. INTRODUCTION

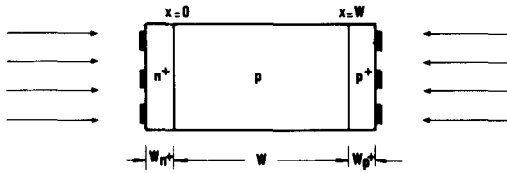
Since the invention of the Back Surface Field (BSF) solar cell [1] Al has been considered as an efficient dopant for manufacturing high quality BSF structures. Al alloyed high-low junctions have also been found very suitable for low-cost automated processing of BSF solar cells [2]. In addition, recent interest has stirred this technology to produce high efficiency MIS-BSF solar cells taking advantage of the low annealing temperature of Al which prevents degradation of the base lifetime [3, 4].

The Double Sided Surface Field (DSSF) solar cell is a

BSF-like structure feasible to be illuminated on both sides as shown in Fig. 1 [5]. The suitability of this device for bifacial illumination was proposed by some of us and coworkers [6]. When front illuminated the behaviour of the DSSF solar cell is similar to that of a BSF cell. The importance of the minority carrier diffusion length in the base ( $L$ ) to base thickness ( $W$ ) ratio and the decisive influence of the effective surface recombination velocity of the high-low junction ( $S_{\text{eff}}$ ) have already been demonstrated [5]. For back illumination the effect of these three parameters ( $L$ ,  $W$  and  $S_{\text{eff}}$ ) in the back illuminated short circuit current rises dramatically since most of the carriers are generated in the proximity of the back surface. Before being collected these carriers have to be effectively reflected by the high-low junction and travel across the whole bulk of the cell. As a consequence the DSSF structure has a higher sensitivity than conventional BSF cells for studying the high-low junction.

The purpose of this paper is to analyse the limits of the Al technology to produce BSF configurations both for monofacial and bifacial illumination. A simple theoretical calculation of the  $I_{sc}$  and  $V_{oc}$  of experimental bifacial structures with Al-doped high-low junctions is presented, including the effects of bifacial illumination and characterizing the high-low junction through an effective surface recombination velocity  $S_{\text{eff}}$ . The relevant technological parameters of a high-low junction depend on the weight of deposited Al and the alloying temperature. In addition to that the purity of the deposited Al strongly influences the diffusion length of minority carriers in the base.

$n^+pp^+$  DSSF solar cells have been fabricated by Al-alloying and  $P$ -diffusion. Histograms of  $L$  vs Al-quality and of  $S_{\text{eff}}$  vs alloying temperature are presented and the results are discussed taking into account the high-low junction model [7] and recent studies of effects occurring in highly doped regions. Our results are compared with experimental results reported by other workers and a discussion of the potential of the Al technology to produce effective high-low junctions is presented.

Fig. 1. Cross section of a  $n^+pp^+$  DSSF Solar cell.

## 2. THEORY

The base contribution to the short-circuit current under front and back illumination ( $I_{scf}$ ,  $I_{scb}$ ) and the base component of the dark saturation current ( $I_0$ ) have all been calculated by solving the continuity equation

$$\frac{d^2 n'}{dx^2} - \frac{n'}{L^2} = \frac{g(x)}{D} \quad (1)$$

The boundary conditions to be considered for short-circuit currents determination are

$$n'(0) = 0 \quad (2)$$

$$-D \frac{dn'}{dx} \Big|_w = S_{eff} n'(W) \quad (3)$$

where  $x=0$  refers to the collecting  $n^+ - p$  junction and  $x=W$  is the  $p - p^+$  high-low junction interface (see Fig. 1).  $L$  and  $D$  are electron diffusion parameters in the  $p$ -base and  $S_{eff}$  is the effective surface recombination velocity of the high-low junction.

The monochromatic generation terms under front and back illumination are

$$g_f(x) = \exp(-\alpha W_{n^+}) \alpha N_{ph} \exp(-\alpha x) \quad (4)$$

$$g_b(x) = \exp(-\alpha W_{p^+}) \alpha N_{ph} \exp[-\alpha(W-x)] \quad (5)$$

where  $N_{ph}$  is the number of impinging photons and  $\alpha$  is the absorption coefficient.

The dark boundary conditions are

$$n'(0) = \frac{n_i^2}{N_A} \left( \exp \frac{qV}{kT} - 1 \right) \quad (6)$$

$$-D \frac{dn'}{dx} \Big|_w = S_{eff} n'(W) \quad (7)$$

and  $g(x) = 0$ .

To calculate the open-circuit voltage the superposition principle is invoked

$$V_{ocf,b} = \frac{kT}{q} \ln \left( \frac{I_{scf,b}}{I_0} + 1 \right) \quad (8)$$

A detailed analysis of the emitter and the  $p^+$ -layer contributions to the short-circuit current has only been carried out by computer simulation [8, 9] which applies only to specific sets of parameters. A considerable amount of work has to be done to adapt this analysis to our case. Therefore we have simply neglected the emitter contribution in our work. This is justified since the only purpose of our calculations is to build up histograms of cells which are classified in categories determined by broad intervals of back to front illuminated short-circuit current ratio.

With respect to the dark current the contribution of

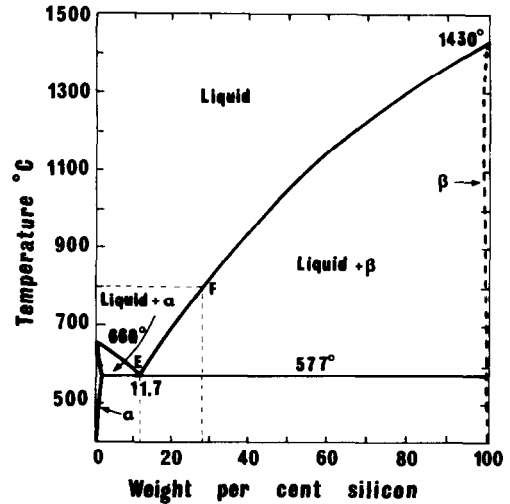


Fig. 2. Phase diagram of the Al-Si binary system.

the emitter has been studied in many recent papers [10, 11]. This component is negligible in our case since the contributions of the base and the  $p^+$  regions are much higher (the last one reflected in the high value of  $S_{eff}$  achieved).

Our base analysis is a low injection analysis. For the base resistivity of our cells (5–8  $\Omega \cdot \text{cm}$ ) high injection is not present as far as the  $V_{oc} \leq 612$  mV as it is our case.

## 3. HIGH-LOW JUNCTION FORMATION

At temperatures above the Al-Si eutectic and below 825°C, which is the range of temperatures used by us, the diffusion of Al atoms into the Si lattice is negligible in a 30' process [12]. However an Al-Si liquid-phase of temperature dependent composition is formed with all the deposited Al and the required amount of Si coming from the crystal. In the Al-Si phase-diagram shown in Fig. 2,  $F$  is the Si weight percentage of the liquid-phase at the alloying temperature. The total weight of Si initially contributing to the formation of the liquid-phase is

$$p_{Al} \frac{F}{100 - F} \quad (9)$$

where  $p_{Al}$  is the weight of deposited Al.

As the sample is slowly pulled out from the furnace the composition of Si in the liquid-phase has to decrease following the liquidus curve of the binary system. The excess silicon segregates at the Si-liquid interface. This recrystallized Si layer is doped at the limit solubility of Al into Si at that particular temperature. When the liquid phase reaches the eutectic composition ( $E$ ) no more Si segregates and the whole liquid solidifies [13].

The net weight of the recrystallized Si is

$$p_{Si} = p_{Al} \left( \frac{F}{100 - F} - \frac{E}{100 - E} \right) \quad (10)$$

and then the thickness of the  $p^+$  layer,  $W_{p^+}$ , can be calculated as

$$W_{p^+} = \frac{p_{Al}}{A \rho_{Si}} \left( \frac{F}{100 - F} - \frac{E}{100 - E} \right) \quad (11)$$

where  $A$  is the area of the sample and  $\rho_{Si}$  refers to the density of silicon.

The formula (10) has been experimentally checked by us by measuring the weight of deposited Al,  $p_{Al}$ , and the weight of the remaining eutectic alloy after the thermal step.

4. EXPERIMENTAL

DSSF solar cell structures have been fabricated on  $\langle 100 \rangle$ , 5-8  $\Omega \cdot \text{cm}$ , 40 mm diameter,  $p$ -type silicon wafers. They were thinned to 100  $\mu\text{m}$  with an alkaline etchant. A phosphorus predeposition was carried out at 875°C during 30' from a  $\text{POCl}_3$  liquid source, giving a  $n^+$  layer of 40  $\Omega/\square$  and a junction depth of 0.3  $\mu\text{m}$ .

Aluminum was evaporated sputtered on one side once the  $p$ - $n$  junction was removed. The sample was then annealed in forming-gas atmosphere at various temperatures ranging from 650 to 825°C during 30'. The amount of deposited Al was tried to keep constant at 0.3  $\text{mgr}/\text{cm}^2$ .

Two qualities of evaporated Al were used: 99% and 99.999% purity. Al and Al-Si eutectic alloy, both 99.995% pure were sputtered from MRC targets. The remaining Al-Si eutectic alloy formed during the annealing step was eliminated by ultrasonic vibration in a 5% HF solution. Sheet resistances between 100 and 500  $\Omega/\square$  were measured.

Measurements of the photogenerated current and open-circuit voltage were made at this stage of the process on 1  $\text{cm}^2$  scribed samples. There are no two-dimensional complications on this measurement [9] and the photogenerated current could be measured under sufficient reverse voltage. Measurement conditions were AM1 and 25°C.

An interpretation of these experiments has been carried out by using the theoretical results of the model developed in Section 2. The reflectivity of bare silicon has been taken from Phillips [14] and the dead layers have been considered 0.3  $\mu\text{m}$  thick.

Our aim was to classify the experimental samples into classes characterized by having  $L$  and  $S_{\text{eff}}$  values comprised in certain intervals. These intervals have been selected to be of nearly equal length in a logarithmic scale, therefore values of  $L$  of 50, 80, 120, 180 and 270  $\mu\text{m}$  and of  $S_{\text{eff}}$  of 100, 300, 1000, 3000 and 10000  $\text{cm}/\text{sec}$  were selected as boundaries of these intervals. In Fig. 3 calculations of  $I_{\text{scb}}/I_{\text{scf}}$ ,  $V_{\text{ocf}}$  and  $V_{\text{ocb}}$  have been carried out for these particular values of  $L$  and  $S_{\text{eff}}$ .

Each sample is characterized by a value of  $L$  and  $S_{\text{eff}}$  which are not known. The measurements of  $I_{\text{scb}}/I_{\text{scf}}$ ,  $V_{\text{ocf}}$  and  $V_{\text{ocb}}$  made for each sample are plotted on a transparent paper. This paper is slid along the  $x$ -axis of Fig. 3 until the three points happen to fall in the same  $L$  interval. When this occurs we associate to the sample the values of  $L$  and  $S_{\text{eff}}$  defined by the intervals in which the three points have been fixed. We have in this way an estimation of the physical parameters governing the performance of every cell.

The cloud of points represented on Fig. 3 is limited by values of diffusion length between 50 and 180  $\mu\text{m}$  and values of  $S_{\text{eff}}$  between  $3 \cdot 10^2$  and  $10^4$   $\text{cm}/\text{sec}$ . Most of the

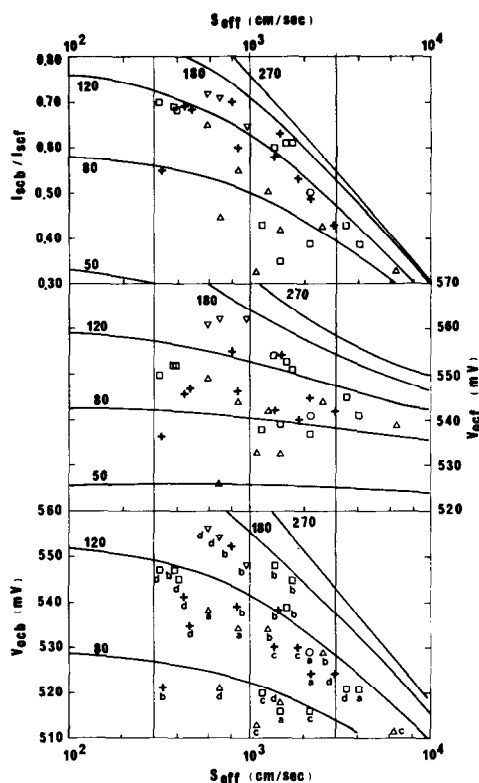


Fig. 3. Diagrams showing the experimental estimation procedure. The theoretical lines are calculations made assuming  $\rho_{\text{base}} = 8\Omega \cdot \text{cm}$ ,  $W_p = 100 \mu\text{m}$  and measurement conditions AM1, 25°C. The experimental symbols refer to the annealing temperature: (O) 650°C, ( $\Delta$ ) 700°C, ( $\square$ ) 750°C, (+) 800°C and ( $\nabla$ ) 825°C; and the Al-quality: (a) evaporated Al 99%, (b) evaporated Al 99.999%, (c) sputtered Al 99.995%, (d) sputtered Al-Si 99.995%.

results are in the area contained by the 80 and 120  $\mu\text{m}$  diffusion length curves and around  $10^3$   $\text{cm}/\text{sec}$  effective surface recombination velocity.

The annealing temperature is expected to influence the effective surface recombination velocity of the high-low junction since the limit solubility [15] and the thickness (see Section 3) increase as the annealing temperature increases. Therefore we build up histograms representing the number of samples which correspond to a certain interval of  $S_{\text{eff}}$  as a function of the annealing temperature. They are presented at the right side of Fig. 4. The influence of the annealing temperature on  $S_{\text{eff}}$  can be clearly appreciated.

The Al quality is thought to affect the minority carrier lifetime in the base. The left side of Fig. 4 displays histograms of the number of samples which correspond to a certain  $L$  interval depending on the quality of the deposited Al. The 99.999% Al statistically shows a better diffusion length than the 99%. About the sputtered material, the Al-Si eutectic alloy seems to be superior than the single Al. This can be perhaps due to the actual purity of the target. The comparison between the 99.999% evaporated Al and the sputtered Al indicates undoubtedly the higher performance of the first. The temperature step involuntarily involved in the deposition process could also justify this difference.

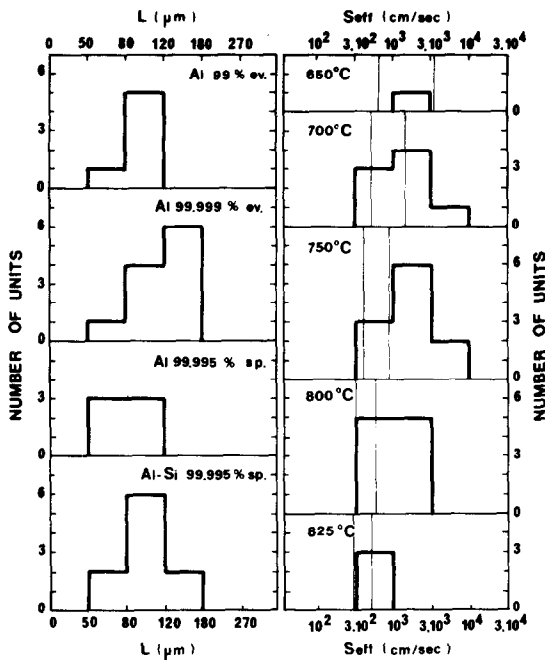


Fig. 4. Histograms representing the number of samples experimentally adscribed to every  $L$  and  $S_{\text{eff}}$  interval as a function of the Al quality and the annealing temperature respectively. On the  $S_{\text{eff}}$  histograms the vertical lines are the theoretical results of Table 1.

### 5. DISCUSSION

Aluminum alloyed high-low junctions have been rejected to fabricate high efficiency BSF solar cells because of the lack of reproducibility [16]. This has been a serious problem during the development of this work and in fact we have been obliged to a statistical interpretation of our results. However from the histograms of Fig. 4 we estimate there is a fundamental limitation of this technology in its conventional way to produce low effective surface recombination velocity. Actually none of the samples has presented a  $S_{\text{eff}}$  below 300 cm/sec. The typical  $S_{\text{eff}}$  value is in the order of  $10^3$  cm/sec.

These experimental conclusions are in rather good agreement with present theoretical models of  $S_{\text{eff}}$  [7] when heavy doping effects are included [17, 18]. In Table 1 numerical values of  $S_{\text{eff}}$  have been calculated assuming a flat profile with the limit solubility concentration corresponding to the alloying temperature and considering a band-gap narrowing through the formula of Slotboom [19]. In the range of impurity levels here studied the formula of Slotboom gives  $\Delta E_g$  values similar to the more refined theoretical model of Lanyon and Tuft [20] and in agreement with the experimental measurements of several authors. As diffusion length of electrons in the  $p^+$ -region we have used  $10 \mu\text{m}$  according with the envelope of best results of Iles and Soclof [21] and in good agreement with measurements of Gudmundsen and Maserkian [22] for good samples. Electron mobility data was taken from [23]. Thickness of the  $p^+$  layer was calculated from the model presented in Section 3 when  $p_{\text{Al}} = 0.3 \text{ mgr/cm}^2$ .

Table 1. Theoretical calculations of  $S_{\text{eff}}$  on  $8 \Omega\text{cm}$  substrate ( $N_A = 3.10^{15} \text{ cm}^{-3}$ ) as a function of the annealing temperature and different  $p^+$ -layers.  $L_p^+ = 10 \mu\text{m}$  in every case

$T_a$ ( $^{\circ}\text{C}$ )	$N_A$ ( $\text{cm}^{-3}$ )	$S_{\text{eff}}$ ( $\text{cm/sec}$ )				
650	$7.5 \times 10^{18}$	669	2440	3456	24	76
700	$8.8 \times 10^{18}$	502	1172	1376	22	72
750	$1.0 \times 10^{19}$	409	794	886	20	69
800	$1.1 \times 10^{19}$	328	545	589	19	67
825	$1.2 \times 10^{19}$	296	469	501	19	65
$S_b$ ( $\text{cm/sec}$ )		$10^5$	$10^6$	$\infty$	$\infty$	$10^4$
$W_p^+$ ( $\mu\text{m}$ )		$0.07 < W_p^+(T_a) < 0.37$ (See Eq. 10 in text)			$\infty$	0.3

The agreement between our experimental estimation of  $S_{\text{eff}}$  of Fig. 4 and the theoretical values is sufficient when the back surface recombination velocity is larger than  $10^5$  cm/sec. Such a high value of  $S_b$  is typical in bare Si and in our case is further justified from the very damaged surface which results from the elimination of the remaining eutectic alloy. The histograms do give worse results than the theory and that can be interpreted by the fact that the effective surface area is increased by the surface roughness produced by selective dissolution of Si in Al during the alloying process. This increases in a proportional way the value of  $S_{\text{eff}}$ . Also our estimation of best results for the diffusion length on the  $p^+$  layer, required for an evaluation of the limits of this technology, tends to give somewhat optimistic theoretical values of  $S_{\text{eff}}$ . The lower limit of  $S_{\text{eff}} \approx 300$  cm/sec for this substrate of  $5-8 \Omega\text{cm}$  ( $N_A = 3.10^{15} \text{ cm}^{-3}$ ) is confirmed.

In the case of BSF solar cells where there is an ohmic contact at the outer surface of the high-low junction the limit of this technology can be obtained by putting  $W_p^+ = \infty$  as made in Table 1. According to our eqn (10) deep junctions need to be fabricated from layers of Al 5 to 20 times thicker than  $W_p^+$ .

The lower the annealing temperature the thicker the Al layer should be. Layers of Al of at least  $20 \mu\text{m}$  have to be used for achieving the condition not very different from  $W_p^+ = \infty$ . Adherence problems are found while evaporating or sputtering heavy layers but this difficulty can be overtaken by using pastes as Tarr *et al.* [3] or screen printing of Al powder as Frisson *et al.* [2].

Selected experimental results reported in the literature and displayed on Table 2 confirm this point. The thin evaporated Al leads to ineffective high-low junctions in comparison with thick film depositions. The best result of Frisson *et al.* [2] has been made by firing a  $25 \mu\text{m}$  thick layer of an Al paste deposited by screen printing [25]. The results can be accurately simulated by the theoretical calculations effectuated in Section 2. When  $L$  is taken as  $800 \mu\text{m}$  and  $S_{\text{eff}} = 20$  cm/sec (see Table 1) and 10% reflection and 10% coverage are assumed,  $I_{sc}$  appears to be  $27.2 \text{ mA/cm}^2$  and  $V_{oc}$  is  $610 \text{ mV}$ .

Table 2. Record of experimental reported results on Al-alloyed BSF solar cells. The extreme right column collects the  $V_{oc}$  data homogenized at  $I_{sc} = 30 \text{ mA/cm}^2$  and  $T = 25^\circ\text{C}$ 

Reference	Structure	Al dep. method	$T_a$ ( $^\circ\text{C}$ )	$I_{sc}$ ( $\text{mA/cm}^2$ )	$V_{oc}$ (mV)	$V_{oc}$ (mV) <sup>†</sup>
Maldekorn et al. [1]	BSF	evaporation	800	35	584	580
Tarr et al. [3]	MIS-BSF	paste	850	30	583	576
Frisson et al. [2]	BSF	powder	780	27.5	609	611
Lindmayer [24]	BSF	evaporation	-	35.3	590	-
This work	DSSF	evaporation	825	26.8*	575	578

†  $I_{sc} = 30 \text{ mA/cm}^2$ ,  $T = 25^\circ\text{C}$

\* Without AR coating

In the case of DSSF solar cells the thickness of the  $p^+$  layer cannot be indefinitely increased since under back illumination the  $p^+$  heavily doped region nearly behaves as a dead layer. Also it cannot be fabricated very thin because in that case the series resistance will be too high. A compromise of these two effects provides a thickness of  $0.3 \mu\text{m}$  like a front diffused  $pn$  junction[18]. In this case a passivation of the outer surface seems to give a surface recombination velocity limited to  $10^4 \text{ cm/sec}$ [11] and hence the lower  $S_{eff}$  which can be expected from these layers as a function of the annealing temperature are recorded in Table 1. It seems to us that such an energetic passivation is very difficult to obtain on the very rough and damaged surface left when the eutectic is eliminated.

The short diffusion lengths reported in this work are due to heavy impurities like Fe, Cu or Zn which are presented in important amounts in the evaporated or sputtered Al material. These are very fast diffusing impurities and during 30' establish a nearly constant impurity concentration all along the bulk of the semiconductor, almost independently of the annealing temperature. This statement has been confirmed by fabricating a structure in the same way as Tarr *et al.*[3], i.e. with a very short annealing time of 40' and a very slow pull out from the furnace. Since the recrystallization of the silicon to form the high-low junction takes place during the cooling of the sample this technique only affects the rapid diffusion of metallic impurities. Results on a  $1 \text{ cm}^2$  (net)  $280 \mu\text{m}$  thick sample alloyed at  $825^\circ\text{C}$  (99.999% Al) are  $I_{scf} = 26.8 \text{ mA}$ ,  $I_{scb} = 7.6 \text{ mA}$ ,  $V_{ocf} = 575 \text{ mV}$  and  $V_{ocb} = 543 \text{ mV}$ , measured at AM1 sun condition and  $25^\circ\text{C}$ . These results can only be explained by means of a diffusion length around  $300 \mu\text{m}$  and a  $S_{eff}$  of  $300 \text{ cm/sec}$ . Longer diffusion lengths,  $\approx 400 \mu\text{m}$ , have been observed to appear on 10–13  $\Omega\text{cm}$  material but essentially the same values of  $S_{eff}$ .

#### 6. CONCLUSIONS

Heavy layers of Al, deposited by thick film techniques and high alloying temperatures of about  $800^\circ\text{C}$ , are required to achieve low  $S_{eff}$  of the  $p^+p$  high-low junc-

tion. Values of about  $20 \text{ cm/sec}$  can be obtained by this procedure on substrates of 5–8  $\Omega\text{cm}$ .

The alloying time must be as short as possible (times of about a minute are enough to allow for the liquid phase formation). In that way the diffusion of impurities contained in the Al is reduced preventing lifetime degradation in the base.

The use of Al alloying techniques for bifacial cells is only feasible if a surface passivation giving a surface recombination velocity not higher than  $10^4 \text{ cm/sec}$  can be achieved. This seems to be difficult due to the bad conditions of the surface obtained after the eutectic layer removal.

*Acknowledgement*—One of the authors (J. del Alamo) is grateful to the IEEE Region 8 Student Activities Committee for the 1st prize that portions of this work have obtained at the 1980 IEEE region 8 Undergraduate Student Paper Contest.

#### REFERENCES

1. J. Mandelkorn and J. H. Lamneck, *Proc. 9th IEEE Phot. Spec. Conf.* Silver Spring, p. 66 (1972).
2. L. Frisson, P. Lauwers, P. Bulteel, L. De Smet, R. Mertens, R. Govaerts and R. van Overstraeten *Proc. 13th IEEE Phot. Spec. Conf. Washington*, p. 590 (1978).
3. N. G. Tarr, D. L. Pulfrey and P. A. Iles, *App. Phys. Lett.* **35**, 258 (1979).
4. N. G. Tarr, D. L. Pulfrey and P. A. Iles, *Proc. 14th IEEE Phot. Spec. Conf.*, San Diego, p. 1345 (1980).
5. A. Luque, J. Eguren and J. del Alamo, *ESSDERC, Montpellier* (1978), *J. Phys. Appl.* **13**, 629 (1978).
6. A. Luque, A. Cuevas and J. Eguren, *Solid-St. Electron.* **21**, 793 (1978).
7. M. P. Godlewski, C. R. Baraona and H. W. Brandhorst, Jr., *Proc. 10th IEEE Phot. Spec. Conf.*, Washington, p. 40 (1973).
8. P. Lauwers, J. van Meerbergen, P. Bulteel, R. Mertens, and R. van Overstraeten, *Solid-St. Electron.* **21**, 747 (1978).
9. C. R. Fang and J. R. Hauser, *Proc. 13th IEEE Phot. Spec. Conf.*, Washington, p. 1318. (1978).
10. M. A. Shibib, F. A. Lindholm and F. Therez, *IEEE Trans. Electron Dev.* **ED-26**, 959 (1979).
11. J. G. Fossum, F. A. Lindholm and M. A. Shibib, *IEEE Trans. Electron Dev.* **ED-26**, 1294 (1979).
12. H. F. Wolf, *Silicon Semiconductor Data*. Pergamon Press, Oxford (1969).

13. F. M. Roberts and E. L. G. Wilkinson, *J. Mat. Sci.* **6**, 189 (1971).
14. W. E. Philips, *Solid-St. Electron.* **15**, 1097 (1972).
15. F. A. Trumbore, *Bell Syst. Techn. J.* **39**, 205 (1960).
16. J. van Meerbergen, J. Nijs, F. D'Hoore, R. Mertens, R. van Overstraeten. *2nd Europ. Phot. Conf.*, Berlin, p. 164 (1979).
17. A. Sinha and S. K. Chattopadhyaya, *IEEE Trans. Electron Dev.* **ED-25**, 1412 (1978).
18. A. Luque, J. Eguren, J. del Alamo, J. M. Ruiz and A. Cuevas, *1st Year Report*, UPM/IES/LS/2880 Spain-U.S. Cooperative Program, Grant. III-P-3008. (April 1980).
19. J. W. Slotboom and H. C. de Graaf, *Solid-St. Electron.* **19**, 857 (1976).
20. H. P. D. Lanyon and R. A. Tuft, *IEEE Trans. Electron Dev.* **ED-76**, 1014 (1979).
21. P. A. Iles and S. I. Soclof, *Proc. 11th Phot. Spec. Conf.*, Scottsdale, p. 19 (1975).
22. R. A. Gudmundsen and J. Maserjian, *J. Appl. Phys.* **28**, 1308 (1957).
23. J. C. Plunkett, J. L. Stone and A. Leu, *Solid St. Electron.* **20**, 447 (1977).
24. J. Lindmayer, *Annual Progress Report*. NSF Grant GI-43090 (Jan. 1975).
25. L. Frisson, Private Communication (March 1980).